Electronic Supplementary Information

Thermal Annealing Reduces Geminate Recombination in TQ1:N2200 All-Polymer Solar Cells

Safakath Karuthedath,[a]* Armantas Melianas,[b†] Zhipeng Kan,[a] Vytenis Pranculis,[c] Markus Wohlfahrt,[a] Jafar I. Khan,[a] Julien Gorenflot,[a] Yuxin Xia,[b] Olle Inganäs,[b] Vidmantas Gulbinas,[c] Martijn Kemerink,[d] and Frédéric Laquai [a]*

[a.] King Abdullah University of Science and Technology (KAUST), KAUST Solar Center (KSC), Physical Sciences and Engineering Division (PSE), Material Science and Engineering Program (MSE), Thuwal 23955-6900, Kingdom of Saudi Arabia.
[b.] Department of Physics, Chemistry and Biology, Biomolecular and Organic Electronics, Center of Organic Electronics (COE), Linköping University, 58183, Linköping , Sweden.
[c.] Center for Physical Sciences and Technology, Savanorių pr. 231, LT-02300 Vilnius, Lithuania.
[d.] Complex Materials and Devices, Department of Physics, Chemistry and Biology, Linköping University, 58183, Linköping, Sweden.
* Corresponding authors E-mail: safakath.karuthedath@kaust.edu.sa, frederic.laquai@kaust.edu.sa
† Present address: Department of Materials Science and Engineering, Stanford University, Stanford, California 94305, USA

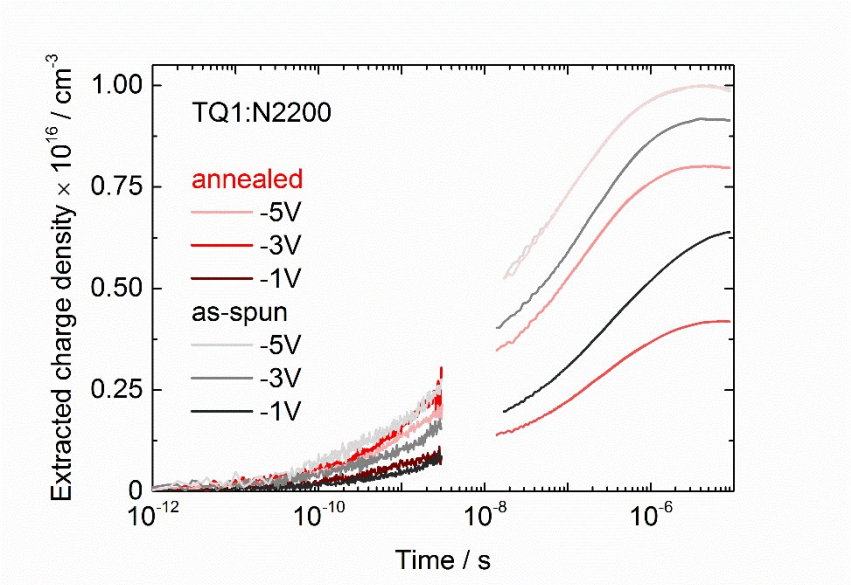

Figure S1. Non-normalized time-resolved charge extraction kinetics in annealed (grey scale) and as-spun (red) TQ1:N2200 OPV devices. The ratio of the total extracted charge at long time delays (t = 9 µs) between the as-spun and annealed samples at U = -1V is equal to 1.52, in good agreement with the corresponding EQE ratio (≈ 1.45) at short-circuit conditions (Figure 1d of the main text). The total amount of extracted charge is less field-dependent in the annealed sample. This correlates well with the FF of both devices, where the as-spun sample has a lower fill factor.

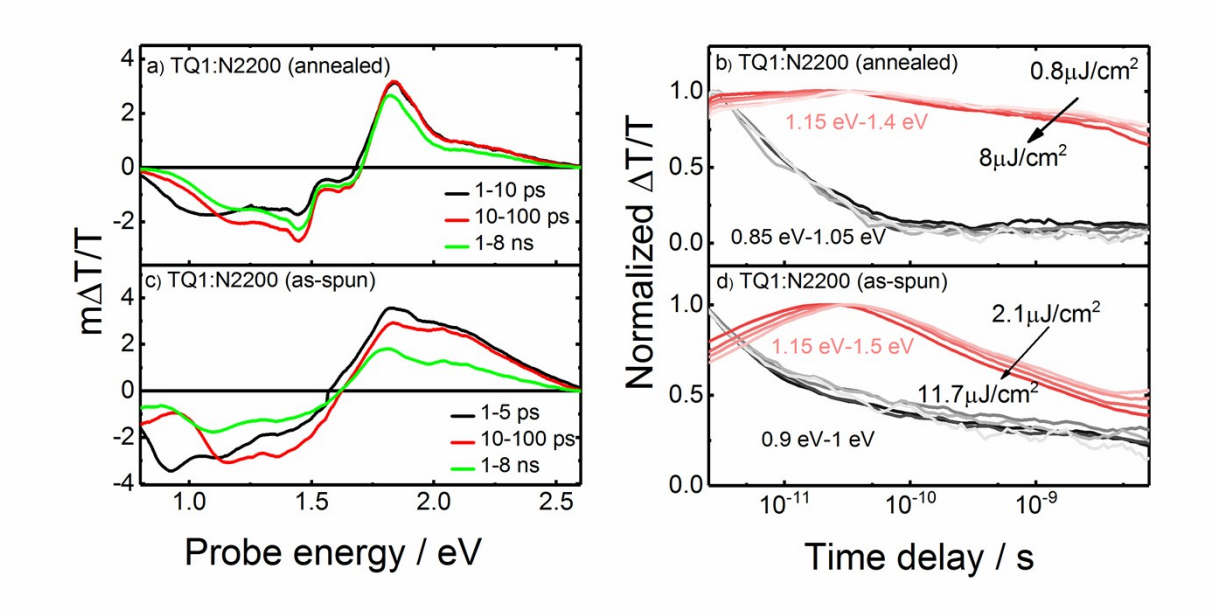

Figure S2. Picosecond-nanosecond TA spectra of **(a)** annealed TQ1:N2200 blends and **(c)** as-spun TQ1:N2200 blends respectively. Picosecond-nanosecond kinetics of the spectral regions ~0.85-1 eV (black lines) and ~1.15-1.4 eV (red lines) of **(b)** annealed TQ1:N2200 and of **(d)** as spun TQ1:N2200 and at different fluences. The gradual increase in the photo-induced absorption at short delay kinetics in panel d (red lines) indicates diffusion-mediated generation in as-spun samples. In the annealed sample (panel b) this process is strongly reduced or even absent.

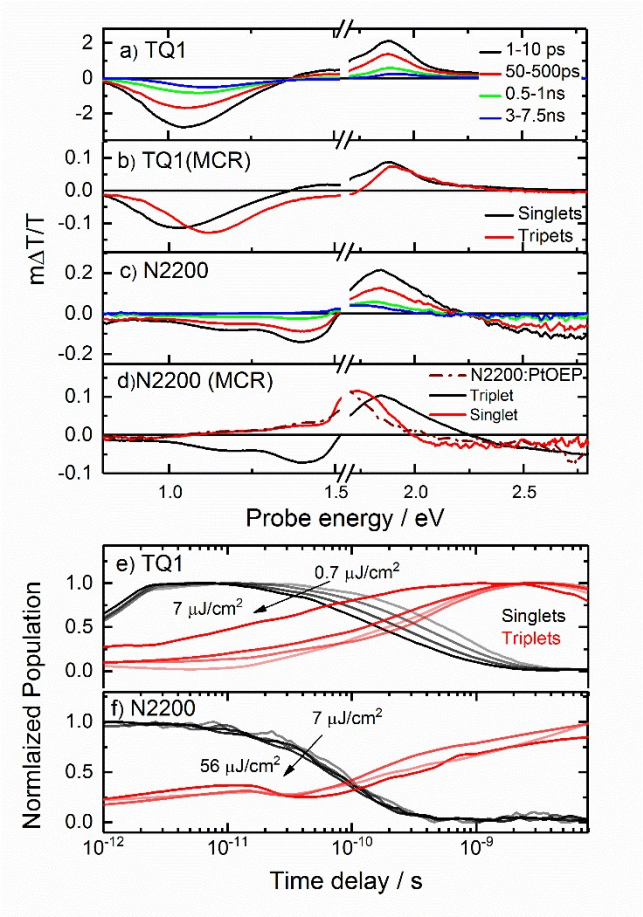

Figure S3. Panel **(a)** and **(c)** show the measured ps-ns TA spectra of pristine TQ1 and N2200 films integrated at different timescales as shown in the legend. A long-lived PA band peaking at 1.12 eV remained even after 8 ns (the longest delay time of our fs-ns TA setup) and was identified as the triplet-induced absorption band of TQ1. Panel **(b)** and **(d)** illustrates the spectra for singlet excitons (black lines) and triplet excitons (red lines) of neat TQ1 and N2200 respectively obtained from MCR analysis. The black in panel **(b)** curve peaking at 1.0 eV is the singlet exciton-induced absorption, while the blue-shifted spectrum peaking at 1.12 eV represents the triplet exciton-induced absorption band which is in agreement with previously reported results. The kinetics of the TQ1 film measured in air are faster compared to the decay dynamics in TQ1 films measured under dynamic vacuum conditions, which supports the assignment of the PA to triplet states in neat TQ1 (See Figure S4). The dashed line in the panel **(d)** is the measured ns-μs TA spectra on N2200:PtOEP blends at 1 μs. The region around 1.5 eV is the region affected by 800 nm white light seed scattering. The red-shift of N2200 TA spectra in panel **(c)** appears to be a consequence of triplet state formation from singlet excitons in this system. We also confirmed the TA spectra by using different white light probes (sapphire vs. CaF2) and detectors (Si vs. InGaAs), see Figure S5. Panel **(e)** and **(f)** shows kinetics of singlets and triplets of pristine TQ1 and N2200 at different fluences obtained from MCR. The absence of a fluence dependence of the singlet exciton decay dynamics of N2200 as shown in panel **(f)** indicates that singlet exciton-exciton annihilation (SSA) is not observed.

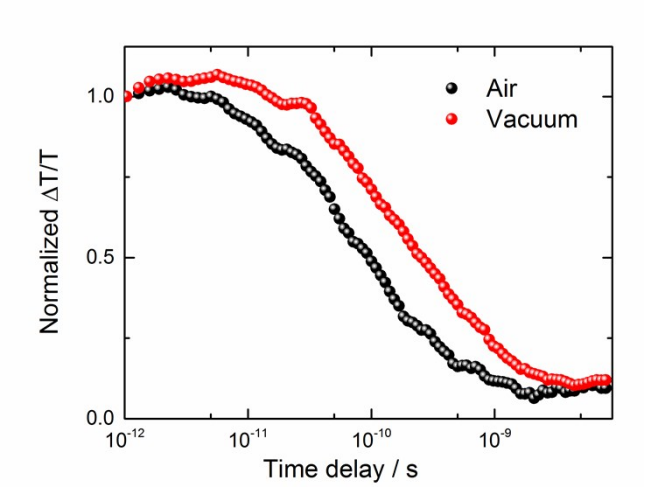

Figure S4. Kinetics of the TA signals of TQ1 in air (black symbols) show a faster decay compared to the kinetics of TQ1 (red symbols) measured under dynamic vacuum conditions, indicating triplet formation in the neat TQ1 films.

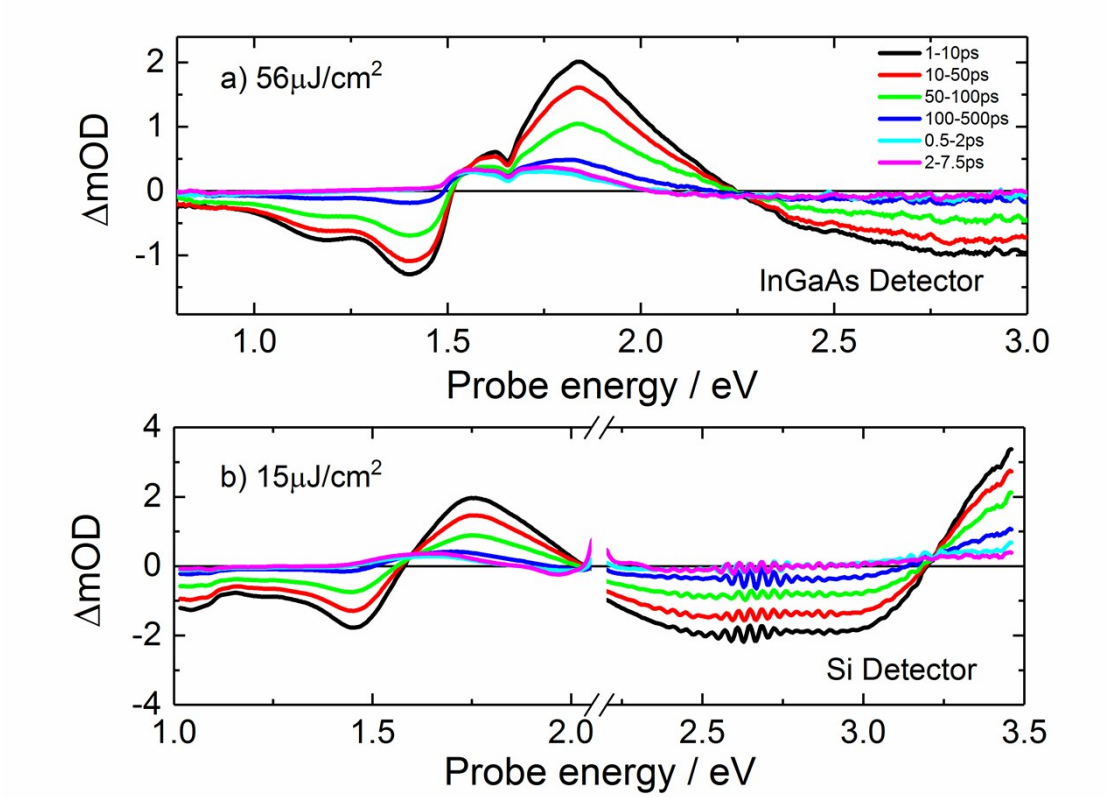

Figure S5. Picosecond-nanosecond TA spectra of a neat N2200 film at different delay times measured under vacuum with an InGaAs detector **(a)** and with a Si-detector **(b)**. These spectra indicate the long-lived states in N2200 films are triplets.

Electronic Supplementary Information

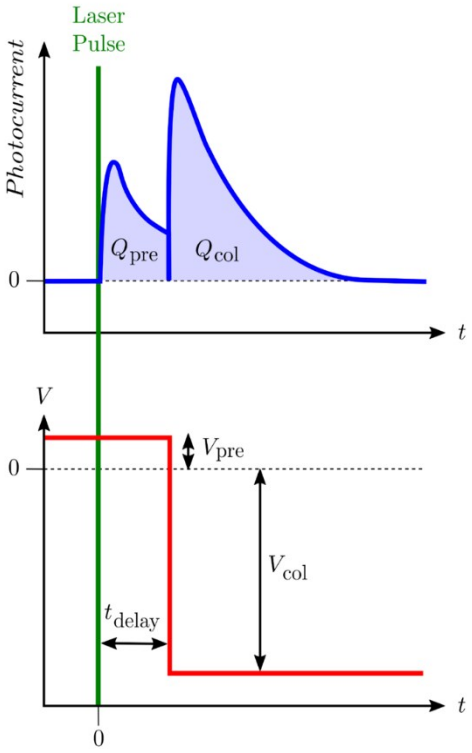

Figure S6. Schematics of the TDCF experiment: photocurrent transients, delay times, applied voltages. In the TDCF measurement, the sample is excited by a laser pulse, while being kept at a constant pre-bias (***V_{pre}***, as shown in the scheme). After a delay time ***t_{delay}***, a rectangular voltage pulse (***V_{coll}***) is applied to extract all remaining carriers, resulting in two photocurrent peaks, one observed after the laser excitation and the other after application of ***V_{coll}***, respectively. The integration of the area under the two curves yields the quantity of charges generated during the laser excitation and extracted before (***Q_{pre}***) (with ***V_{pre}*** applied) and during (***Q_{col}***), that is, the application of the collection field, respectively. The sum of ***Q_{pre}*** and ***Q_{col}*** reveals the total number of generated charges ***Q_{tot}***.

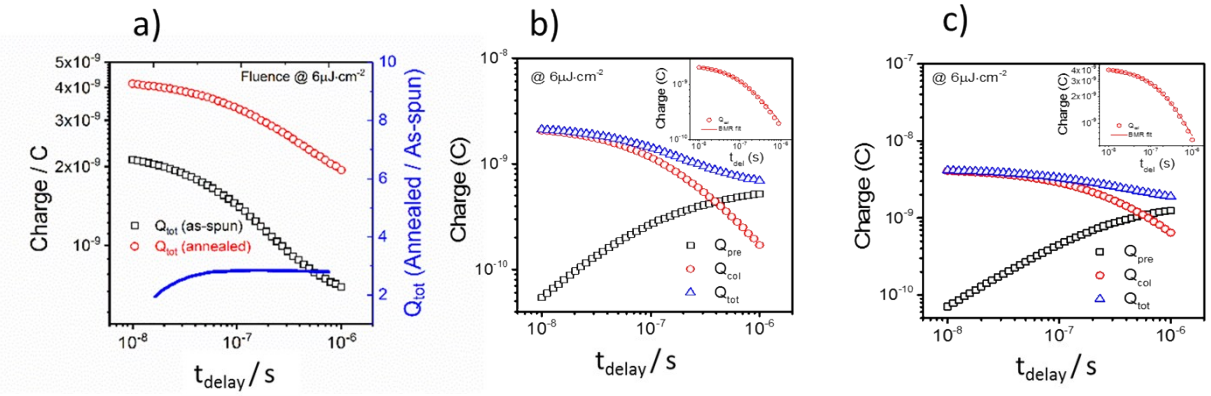

Figure S7. Data from TDCF measurements: a) Total charge, Q_{tot}, extracted from as-spun (black squares) TQ1:N2200 devices and annealed (red circle) TQ1:N2200 devices. The fluence used here was 6 μJ/cm^2. The blue solid line indicates the ratio of charge carriers extracted from the annealed and as-spun samples. Charge extracted prior to and after application of the collection field and total extracted charge as function of ***t_{delay}*** for b) as-spun and c) annealed active layers, respectively. The insets show the fit of Q_{col} to a bimolecular recombination model, which yields the β_{TDCF} shown in table 1.

Electronic Supplementary Information

Table S1. N_0 obtained from the two-pool model fits to the carrier recombination dynamics using an initial carrier concentration as starting point estimated from the absorption of photons for each fluence for both annealed and as-spun samples.

Fluence	Annealed TQ1:N2200	Fluence	As-spun TQ1:N2200
21 μJ/cm^2	1×10^{18} cm^{-3}	60 μJ/cm^2	5.5×10^{18} cm^{-3}
14 μJ/cm^2	6.1×10^{17} cm^{-3}	45 μJ/cm^2	4.5×10^{18} cm^{-3}
8 μJ/cm^2	4.1×10^{17} cm^{-3}	30 μJ/cm^2	3.4×10^{18} cm^{-3}
4 μJ/cm^2	2.3×10^{17} cm^{-3}	15 μJ/cm^2	2.2×10^{18} cm^{-3}

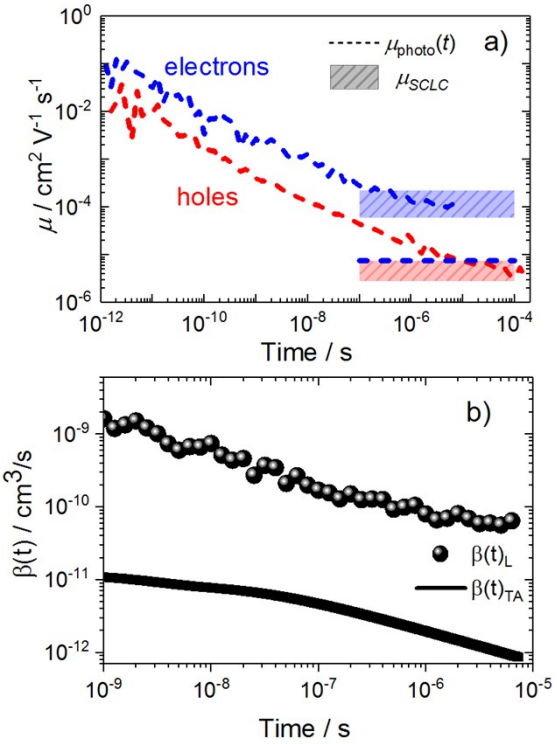

Figure S8: a) Time dependent mobility in TQ1:N2200 solar cells obtained from TREFISH and TPC measurements (dashed lines) for electrons and holes, respectively. Steady-state mobility obtained from SCLC measurements are shown as shaded rectangles. b) Time dependent Langevin recombination coefficient (symbols) for TQ1:N2200 devices calculated from the time dependent mobilities obtained from transient photocurrent measurements using: $\beta(t) = \frac{q}{\varepsilon_0 \varepsilon_r}(\mu_h(t) + \mu_e(t))$, where $\beta(t)$ is the Langevin recombination coefficient, q the elementary charge, $\mu_h and\, \mu_e$ are the hole and electron mobilities, respectively, and ε_0 and ε_r are the vacuum permittivity and dielectric constant (absolute permittivity) of the sample. Both samples show similar mobilities (see Figure 2 in the manuscript) hence, the calculated Langevin recombination coefficient for both annealed and as-spun samples are the same. The solid line in panel (b) indicates the bimolecular recombination coefficient calculated from TA data.